Abstract

Over the course of the project, a gain scheduled controller was successfully designed using Matlab and Simulink. The controller has an operating range of 15-40°C. The most probable reason for its inability to operate between 5-15°C could be due to parameter uncertainties in the plant model. The controller was able to reject disturbances (such as sudden rise in ambient temperatures) and bring the chamber back to the desired temperature. The controller was able to achieve a response having less than 20% overshoot and absolute error less than 2°C. The controller was able to give response with 0% overshoot and 0 steady-state error. The controller was also able to compensate for errors due to disturbances successfully.

A mathematical model of the system was also successfully designed, simulated, verified and validated using Simulink. An actual physical hardware of the heating/cooling system (without a controller) was developed to verify the behavior of the plant. The model was able to correctly represent a general heating/cooling system. A maximum absolute error of 6°C and minimum error of 0.2°C were obtained during the validation stage of the model. Furthermore, a list of suggestions for expanding the capabilities of GUSTAVO have also been included in section 6.

Contents

List of Figures

Tables

List of Abbreviations & Symbols

1. TEM – Thermoelectric Module
2. EMF – Electromotive Force
3. PCR – Polymerase Chain Reaction
4. T_{in} – Temperature inside heating/cooling chamber
5. T_{amb} – Ambient temperature
6. Q_T – Rate of change of energy on top side of thermoelectric module
7. Q_B- Rate of change of energy on bottom side of thermoelectric module
8. T_T – Temperature of top side of thermoelectric module
9. T_B - Temperature of bottom side of thermoelectric module
10. S_m – Seebeck Coefficient
11. R_m – Thermoelectric module resistance
12. K_m – Thermal conductivity of thermoelectric material
13. Q_P – Heat absorbed due to peltier effect
14. $Q_f^{B \to T}$ – Heat due to fourier heat conduction from bottom surface to top surface of thermoelectric material.

1 Introduction

1.1 Thermoelectric Devices and its Relevance

Thermoelectric devices are being used extensively for various applications. From smartwatches to satellites, thermoelectric devices have found their way into our lives, often going unnoticed. These versatile devices can be used to heat, cool and even generate electricity [1], which scientists and engineers have found multiple ways to exploit for different purposes. Some of the common applications that we see in our day-to-day lives include powering smartwatches using body temperature, portable coolers, car seat ventilation, and for cooling applications in laboratory [2]. These are also used in space applications, one of the best examples being radioisotope thermoelectric generators [3] that was used to power the Voyager-1 and Voyager-2, both of which entered interstellar space recently.

TEMs, as they are often called, however, are highly non-linear [4] which makes it extremely challenging to design controllers for precise temperature control. However, their advantages such as compactness, absence of moving parts, minimal maintenance, quick response and not requiring any refrigerants [5] outweigh its disadvantages. These advantages are why they are being for many applications as listed above. Therefore, thermoelectric control is a pivotal field of research which can open arenas to a wide range of applications, especially if we could design a controller to operate the thermoelectric plant at optimal efficiency and performance.

1.2 Previous Work

There are numerous literature with respect to modelling a thermoelectric plant and design of a thermoelectric control system. [6] illustrates designing a PID controller for the purpose. The author experimented with multiple TEM modules connected in series and in parallel, and compared their results in this article. Although it served as a good starting point to understanding a thermoelectric control system, it lacked analysis on how to model and linearize the plant, and what assumptions were considered in the model. These are crucial points for a reader to get an understanding of the challenges that lie in designing a controller for a thermoelectric system. [4] discusses a small signal linearized model of a thermoelectric plant. The author has also provided a summary on the fundamental principles of a TEM device and builds up on it to derive the differential equations for the hot and cold surfaces. Moreover, the paper also provides hints to what reasonable assumptions can be made so that a simple model of the plant can be obtained. However, there is not much information on how the transfer function of the system was obtained, which again is crucial for designing a controller. [7] [8] [9] served as excellent resources to gain a wider understanding about how TEMs are being used and the principles behind its working. [10] [1] [11] have excellent details on the internal workings of a thermoelectric device, how to derive the differential equations of the top and bottom surfaces from their energy balance equations, and how to go about modelling a thermoelectric cooler or generator. These books could be used a main source of reference for a deeper understanding in the mechanics of TEM. In [12] [13], electrical equivalent of a TEM system has been described, which facilitates plant modelling for electronic engineers who may not have much background in thermodynamics and heat transfer. However, the fundamentals of heat transfer and its modelling have been explained in detail in [14] [15] and a some form of understanding the subject is crucial to design high fidelity models. It will also pay-off while verifying and validating the plant model. [12] also includes an experimentally validated method to obtain approximated values for seebeck coefficient, electrical resistance and thermal conductivity of TEM using its parameters from datasheet. This would enable us to develop a linear control system for controlling temperature with TEM.

In [16], a non-linear control system called sliding mode control was developed for a pcr thermal cycler using TEM. The article has clearly explained how to model a thermoelectric pcr thermal cycler and how to design a non-linear control for it. Although this type of controller has the added advantages of being able to work in a larger range of temperatures, and its robustness to variations in parameters, a sliding mode control is often complicated to design and analyse, requiring a knowledge of non-linear analysis methods such as Lyapunov stability analysis [17]. On the contrary, linear system design has a wide variety of methods for analysis and design, and is well established in industry, making linear system design an attractive option to consider. Other notable works in control design for TEM include [18] in which a fuzzy adaptive PID control was designed.

In all the previous work mentioned above, the differential equation describing the change in temperature inside the chamber was not derived. The controlled temperature was that of one of the ceramic surfaces of the TEM. This project takes into account the dynamics of the temperature inside the chamber, T_{in} and use this as the control variable. A gain scheduled controller was also opted due to its robustness against uncertain parameters and its simplicity in design, given the limited time available for the project.

The designed system would pave the way for developing a microplate heater/cooler sub-system as a new functionality for a liquid handling robot called GUSTAVO (Glasgow University

ScienTific Automated Volume O-tron). GUSTAVO is an affordable liquid handling robot for biomedical applications that was developed by James Campbell, Jake Beveridge, Tara Duggan and Ross McKeown, under the supervision of Professor Nikolaj Gadegaard at University of Glasgow. It is based on the open source FINDUS (Fully Integrable Non-commercial Dispensing Utility System) project [19].

1.3 Chapter Organization

This report is a comprehensive coverage of the various processes that had gone into developing a model of a thermoelectric heating and cooling system, and designing a gain scheduled controller for it. The report also has an extensive analysis of the results that were obtained in running the simulations.

Section 1 introduces the reader to the concept of thermoelectricity, feedback control and the fundamental principles that drive a thermoelectric device. It also gives the reader a glimpse into the challenges in modelling the system and designing a controller for it. Furthermore, It also summarizes some of the previous work that had been done in modelling the system and designing a controller for it.

Section 2 discusses the theoretical background behind thermoelectric effect and gain scheduled control. It provides a basis for the rest of the report.

Section 3 depicts the process flow that was followed over the course of the project.

Section 4 presents the design and analysis that had gone into developing a simulation of the control system for the thermoelectric cooler and heater. The differential equations that describe the change in temperatures of the chamber and the TEM surface is derived in this section of the report.

Section 5 details out the results obtained from simulating the heater/cooler control system in Matlab and Simulink. It covers an in-depth analysis of the results for various scenarios such response in presence of disturbances, response during heating and response during cooling to name a few.

Section 6 provides recommendations for what could be done in the future which includes new useful features for GUSTAVO and in improving the control system for thermoelectric heater and cooler. These suggestions are a result of evolution of the understanding about the system during the time of the project which will definitely be worthwhile to try out in the future.

2 Theoretical Background

2.1 Thermoelectric Cooling & Heating

Thermoelectric effect is the phenomenon of generating electricity through temperature gradient and vice versa [10]. Hence, thermoelectric devices are commonly referred to as a thermoelectric heat pump or a thermoelectric generator. The latter is beyond the scope of this report. Although most of the theory described in this section is related to thermoelectric heat pumps - devices that 'transport' heat from end to the other when external work (electric current) is done - they also apply to thermoelectric generators. In doing so, the temperature of the volume of space from which heat is removed turns cold while the other turns hot, leading to a temperature differential [1]. Therefore, as part of the project, the TEMs were considered to be a heat pump for which, a controller was designed to drive a volume of space to a desired temperature. There are three fundamental principles that enable thermoelectric effect: Peltier effect, Seebeck Effect and Thomson Effect [20]. The imapct due to Thomson effect is negligible [4] and hence was not used in the modelling the system .

A thermoelectric module basically consists of p and n doped semiconductors connected electrically in series and thermally in parallel. Hence, each p-n pair form a thermocouple in the module. Figure 1 illustrates the basic working of a TEM cooler using a single p-n pair. When a voltage is applied to the pair as shown in the figure, heat (Q_T) is absorbed from the top surface of the module, leaving that surface cold. This heat is 'pumped' to the bottom surface (Q_B) and released out, leaving this surface warm. When the polarity of voltage is reversed, the top surface becomes warm and the bottom surface becomes cold. Hence, by reversing the polarity, a TEM can be used as a heater or a cooler.

However, for effective cooling, multiple p-n thermocouple pairs are sandwiched between two ceramic plates as shown in figure 2.

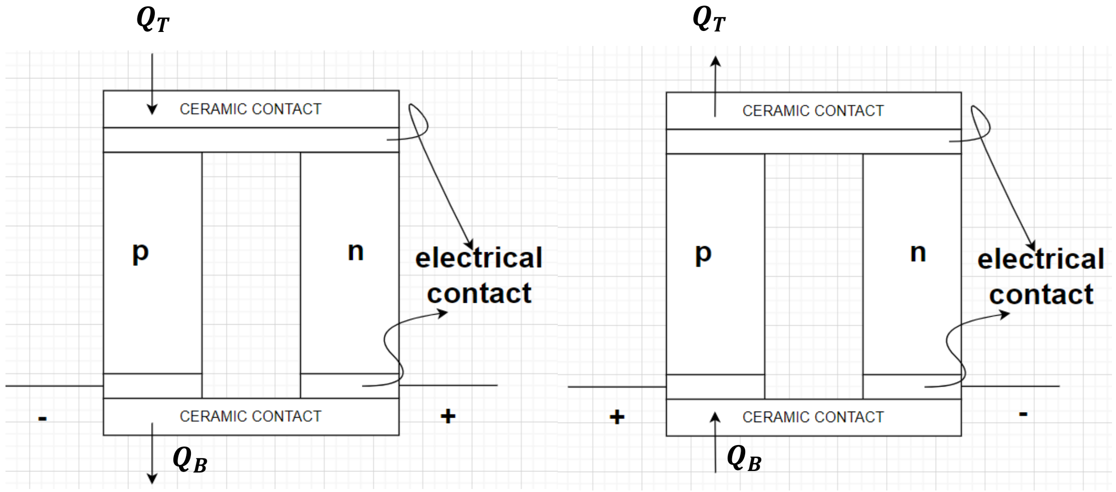

Figure 1: Left schematic depicts heat flow when operating as a cooler. Right schematic depicts heat flow when operating as a heater by changing polarity of voltage supply

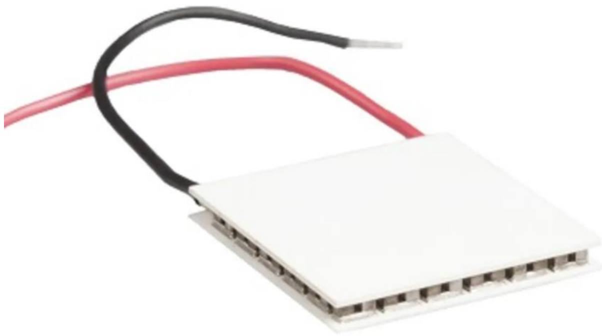

Figure 2: Actual thermoelectric module with multiple p-n thermocouples sandwiched between ceramic plates. The white surface on top and bottom are the ceramic plates

The absorbing of heat at the cold surface of the module when excited by an electric current is called Peltier Effect [20]. The heat absorbed is proportional to the current applied. Hence, the heat absorbed at the cold end of TEM can be defined as [10]

$$Q_{Peltier} = \pi I \quad \text{----------} \; \textit{Equation 1}$$

where π is the Peltier coefficient and I is the current applied.

Seebeck effect refers to the generation of an EMF across the terminals of the thermoelectric module when a temperature gradient develops across the opposite faces [10]. This is the basic principle behind thermoelectric generation. Hence, the voltage that is being supplied externally must work against the seebeck voltage in order to pump heat. The EMF developed is directly proportional to temperature gradient. The Seebeck coefficient (S_m) is defined as [10]

$$S_m = \frac{\Delta V}{\Delta T} \text{ ---------- } \textit{Equation 2}$$

Where ΔV is the emf generated across the terminals of thermoelectric module and ΔT is the difference between the temperatures of the top and bottom surfaces of the thermoelectric module.

2.2 Feedback Control

Controllers are used to provide the necessary actuation to output a desired signal, given a set of specifications [15]. One of the most common controllers used in industry is the PID (Proportional Integral and Derivative) controller which has proved its versatility over the years, even in the presence of other advanced control laws [21]. What makes PIDs attractive is its simplicity in both analysis and design [21]. One of the most common approaches in control design is to design a PID controller first as it is known for a fact that it might just work.
Controllers can be open-loop or closed loop/feedback control. As part of this project, a closed loop control system was designed to meet the design specifications [22].

A feedback controller measures the controlled output variable in order to determine the necessary control action . Hence, it delivers the appropriate control signal based on the error between the desired and the actual output [23]. A reference $r(t)$ is provided as input to the feedback system which is the signal we desire to get at the output of the system. Figure 3 shows the basic structure of a closed loop control system.

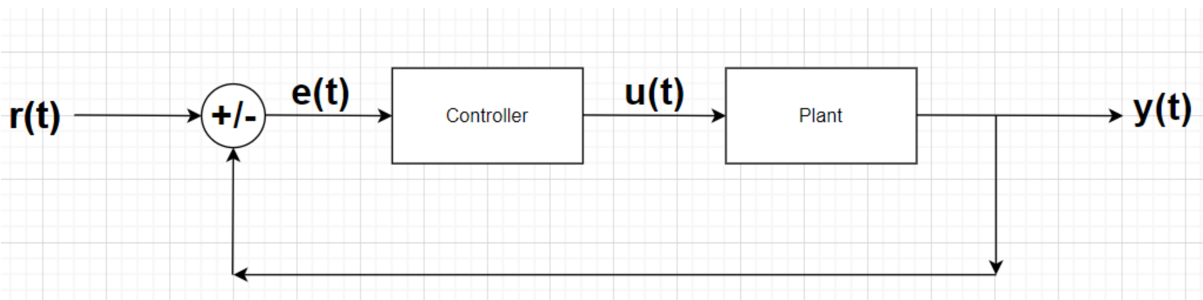

Figure 3: Closed Loop Control

Figure 3 demonstrates a negative unity feedback controller. In the figure, $r(t)$ corresponds to the reference input, $e(t) = r(t) - y(t)$ corresponds to the error between the output and the reference, $u(t)$ corresponds to the control signal, and finally $y(t)$ is the output of the system. One of the most popular forms of control analysis is the classical control theory which utilizes Laplace transform which is used to analyze the system and signals in the frequency domain (or s-domain). Figure 4 depicts a feedback control in the s-domain.

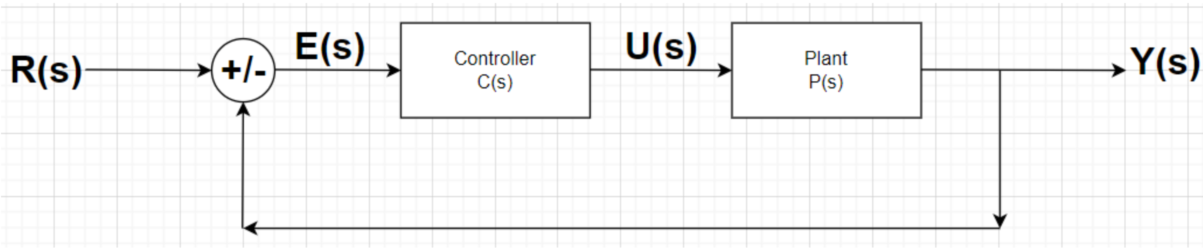

Figure 4: Closed Loop Control in Laplace Domain

In order to analyze the system, the transfer function of the system is obtained as shown in equation (for a negative feedback closed loop system) [21]:

$$T(s) = \frac{Y(s)}{R(s)} = \frac{P(s)C(s)}{1+P(s)C(s)} \text{ ---------- } \textit{Equation 3}$$

Compared to open-loop control systems, feedback control brings many advantages such as disturbance rejection, good reference tracking and reducing sensitivity to plant uncertainties [23]. The thermoelectric heating/cooling plant that was used for the project suffer from parameter uncertainties [24] and disturbances from ambient. Hence it is clear why a feedback control is the right choice for the application.

2.3 Gain Scheduled Control

A non-linear controller called gain scheduled controller was designed to control the temperature inside the enclosure. It is a robust controller which could be applied to non-linear systems whose dynamics keep changing [25]. They are basically a set of linear controllers such as PID controllers tuned at various operating points. The controller selects appropriate gains based on its current operating point. A common approach is to use a lookup table that has keys as the scheduling variable and the values as the required gains for that value of scheduling variable [26]. The control system designed as part of this project also follows the same approach. Figure 5 illustrates a high level structure of a gain scheduled control system.

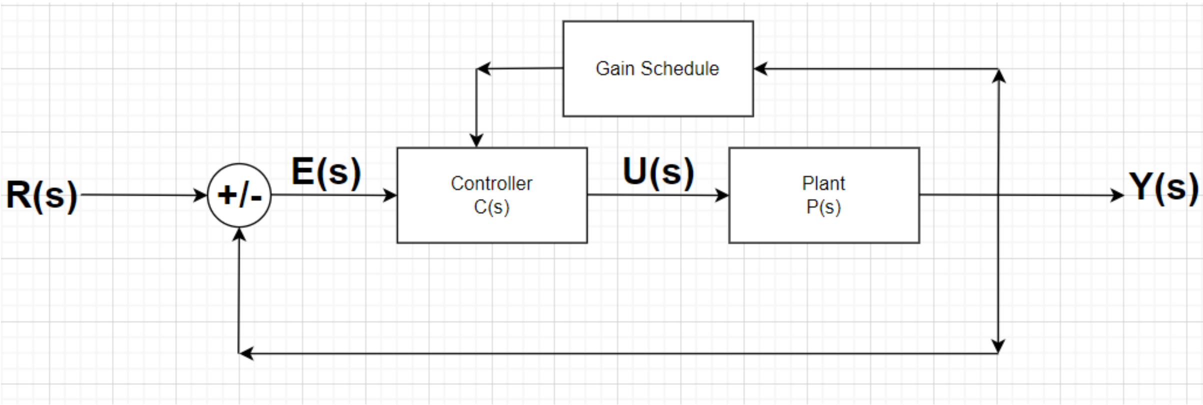

Figure 5: Block Diagram of Gain Scheduled Control

The gain schedule sub-component in the figure checks the current operating region of the system from output and updates the gains of the controller based on this. By referencing the lookup table, the controller will know what gain is to be used for proper functioning of the system in the current operating region.

2.4 Challenges in controlling a TEM

Let $\frac{dQ_T}{dt} = m_T c_T \left(\frac{dT_T}{dt}\right)$ and $\frac{dQ_B}{dt} = m_B c_B \left(\frac{dT_B}{dt}\right)$ denote the change in energy at the top and bottom surfaces of thermoelectric module. Assume that the temperature of the top surface drops while that of the bottom increases. Then the differential equation describing the change in temperature in the top and bottom surfaces of the thermoelectric module can be given as [10]

$$m_T c_T \left(\frac{dT_T}{dt}\right) = n\left(S_m I T_T - \frac{1}{2} I^2 R_m - K_m (T_B - T_T)\right) \text{ ---------- } \textit{Equation 4}$$

$$m_B c_B \left(\frac{dT_B}{dt}\right) = n\left(S_m I T_B + \frac{1}{2} I^2 R_m - K_m (T_B - T_T)\right) \text{ ---------- } \textit{Equation 5}$$

where n is the number of thermocouple pairs inside the thermoelectric module, $m_B c_B$ and $m_T c_T$ are the mass and specific heat capacities of the bottom and top surfaces of thermoelectric module respectively.

The challenge in designing a controller for a TEM lies in the fact that it highly non-linear due to the I^2 term and the module's temperature dependent parameters ($S_m, K_m \; and \; R_m$) [24]. S_m is the seebeck coefficient, R_m is the thermoelectric module resistance and K_m is the thermal conductivity of the thermoelectric module.

Therefore, a robust control system is required to bring the system to a desired temperature. A robust controller remains immune to plant parameter changes and uncertainties, and hence aids in obtaining the desired temperature.

3 Design Process Flow:

The following flowchart illustrates the process flow that was followed in designing the controller over the course of the project.

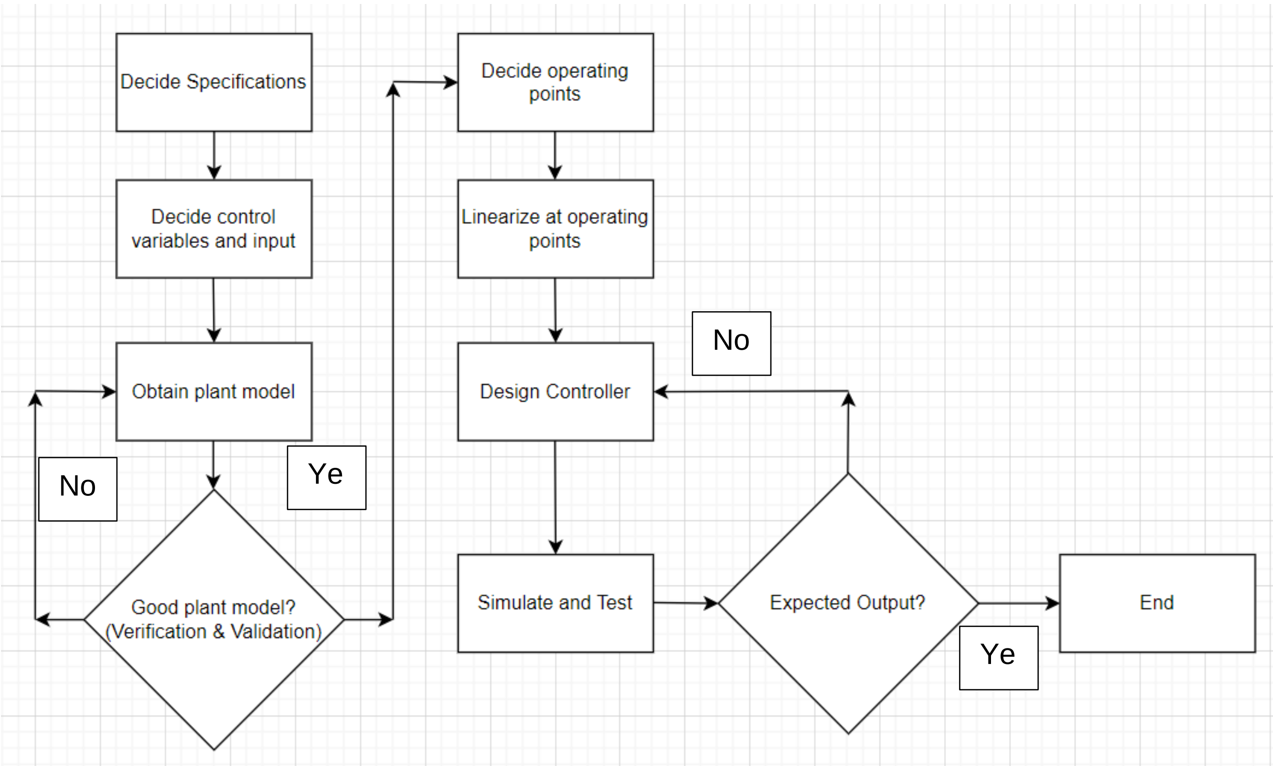

Figure 6: Flowchart of Design Process Flow

4 Design and Implementation

Figure 7 shows a schematic of the system that was modelled in Matlab. Figures 8 and 9 displays the actual hardware that was developed to test the fidelity of the model. The term ‘plant’ refers to the system to be controlled due to its widespread adoption in the controls community.

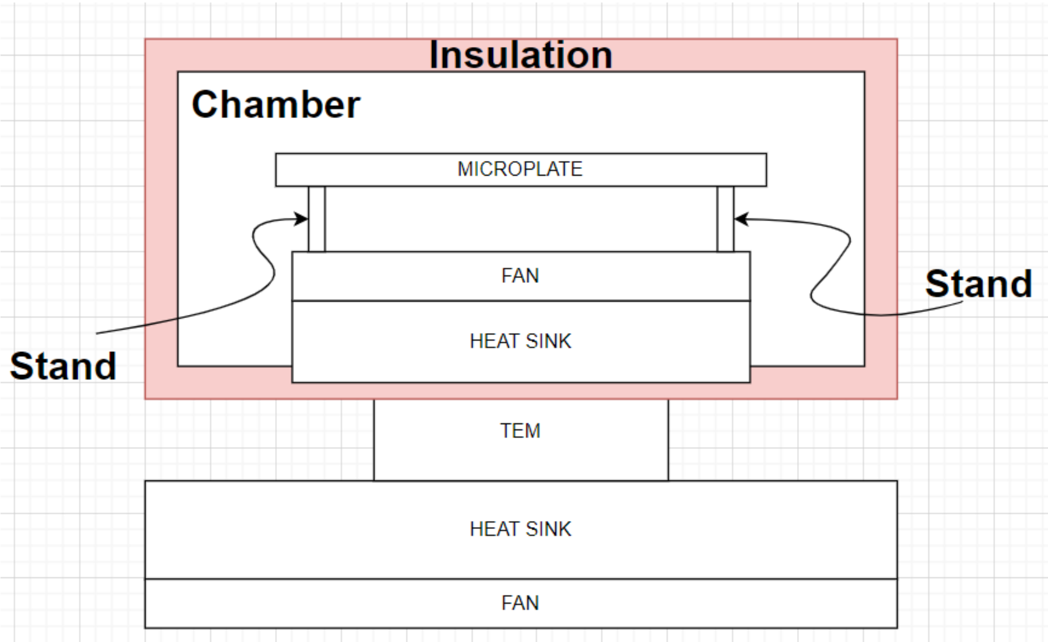

Figure 7: Schematic of Thermoelectric Heater/Cooler Plant

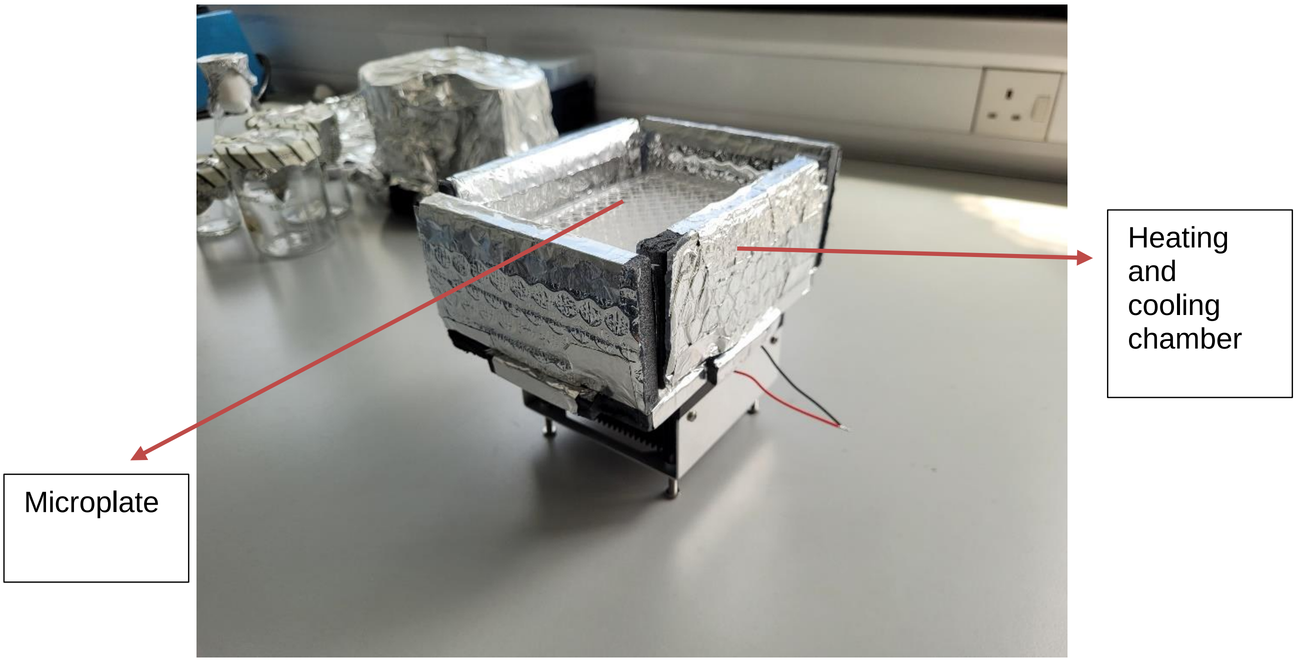

Figure 8 : Actual hardware built for model validation

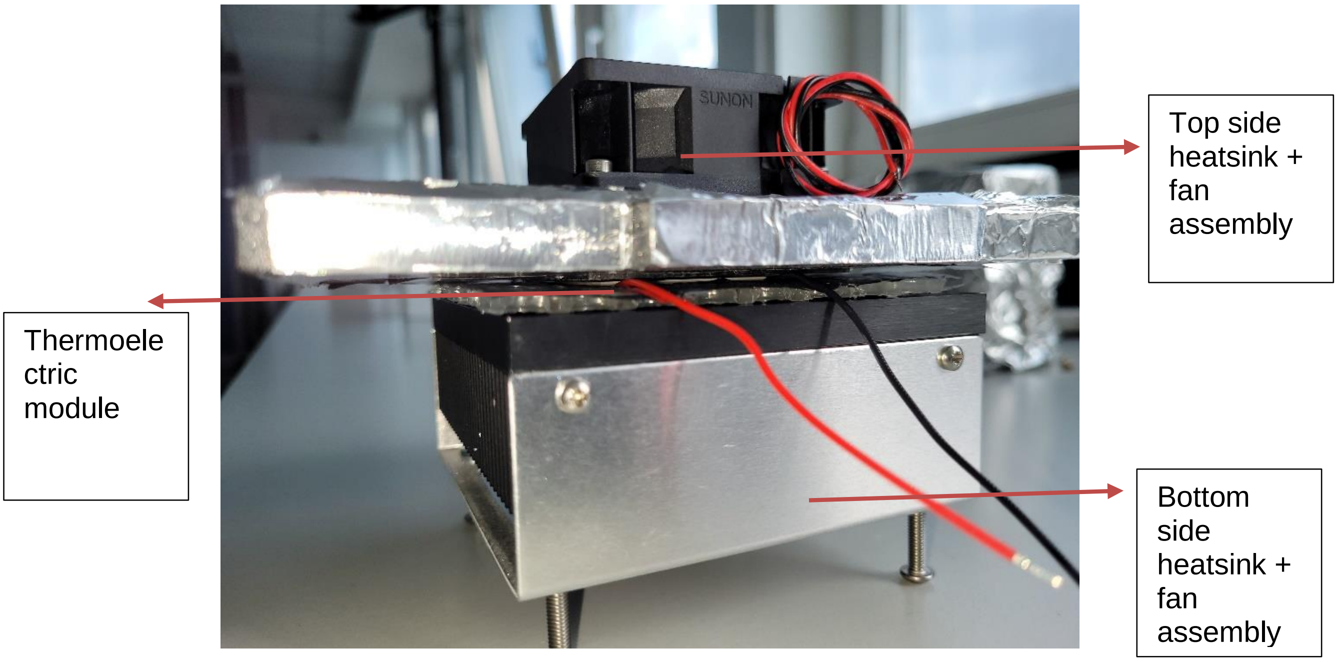

Figure 9 : Different parts of the hardware (Walls removed)

4.1 Model Description

The plant consists of the following parts:

- Top side heatsink + fan assembly
- The microplate that needs to be cooled (through ambient cooling)
- Thermoelectric module (TEM)
- Bottom side heatsink + fan assembly
- Chamber

The chamber was made from Extruded Polystyrene which has very low thermal conductivity (≈0.1 W/m℃). However, to ensure minimal heat leakage through the walls and gaps, the chamber was clad in a thermal foil which reflects any heat trying to enter through the walls, hence helping to maintain the temperature inside, and reduce disturbances for the controller to compensate. An opening was made on the base of the chamber for fixing the thermoelectric module. The heatsink+fan assembly were attached to the ceramic surface of the module using a thermal glue.

Heatsinks play a crucial role in the plant. It is recommended to have a heatsink and a blower fan attached to it for maximum cooling and heating efficiency through forced convection [10]. Failure to add a heatsink could overheat the warm side of the thermoelectric module, which eventually leads to system failure. Moreover, it could also lead to heat leaking into the cold side of the module, which could reduce the plant's overall effectiveness [10]. In order to prevent any heat from leaking into the chamber, the thermoelectric module was placed in such a way that one ceramic face of the module is inserted completely inside the chamber while the rest of the module is exposed to ambient. To further reduce heat leakage from the hot side heatsink and the hot side of the module, the module was also surrounded by a thermal foil, exposing only the ceramic top and bottom as shown in figure 10. Table 1 lists the technical specifications of the TEM that was used for the project [27]:

$I_{maximum}$ (A)	6
$V_{maximum}$ (V)	15.7
$P_{maximum}$ (W)	55.6
$\Delta T_{maximum}$(°C)	74

Table 1: Thermoelectric module maximum parameters

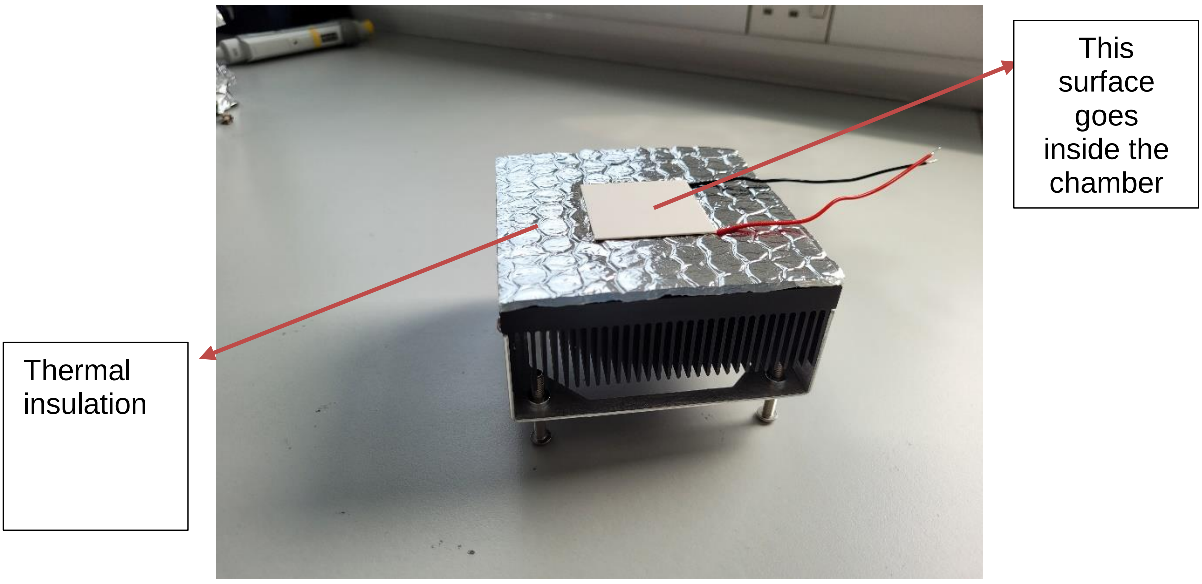

Figure 10: Base layer thermal insulation

4.2 Mathematical Model of the System

In order to describe how the system behaves, differential equations of three separate parts of the plant was derived:

- Temperature inside the chamber (T_{in})
- Temperature of top side of thermoelectric module (T_T)
- Temperature of bottom side of thermoelectric module (T_B)

The differential equations tell us how T_{in}, T_T and T_B change due to the heat exchange that takes place between different components of the plant and the ambient.

Heat can be exchanged from one medium to another through three different processes, namely conduction, convection and radiation. In order to simply the analysis and modelling, the effects of radiation were not considered in the project.

Conduction is the process of heat transfer from hotter end of an object to the colder end due to the gradient in temperature between the two ends [28]. The one-dimensional rate of heat transfer through conduction is governed by Fourier's law of thermal conduction

$$\frac{dQ_{cond}}{dt} = -\frac{K_m A(T_h - T_c)}{L} \text{ ---------- } \textit{Equation 6}$$

Where K_m is the thermal conductivity of the object, A is the cross-sectional area perpendicular to the direction of heat flux, L is the length of the solid along which heat is transferred, T_h is the temperature of the hot side of the object and T_c is the temperature of the cold side of the object.

With respect to the plant, conduction of heat takes place between the two ceramic plates of the thermoelectric module, through the p-n thermocouples sandwiched between them.

Convection is the transfer of heat within fluids [28]. This could take place in the form of forced convection – where fluid like is forced to move recirculate - and free convection – due to natural movement of fluid particles. The plant that was designed for the project utilizes forced convection on both, top side and the bottom side of the module through a heatsink and fan assembly.

The equations derived in this section assumes that the plant is being operated as a cooler. The procedure will be the same for a heater, except for a few reversal in the signs of heat being exchanged.

4.2.1 Modelling Variation of T_{in}

Consider T_{in} to be the temperature inside the chamber where the microplate is to be kept. This is the temperature that needs to be controlled. Let Q_L be the heat that is pumped out from the chamber by the TEM + heatsink + fan assembly. To simplify the model and analysis, the chamber in fig was considered as a box with five walls insulated. The other wall (base wall) which is attached to the heatsink + TEM assembly is not insulated. Hence, the base wall was considered to be made of the material of the heatsink. Hence, there is Q_{leak} coming in to the chamber through the five insulated walls and Q_L being pumped out by the heatsink.

$$Q_L = \frac{(T_{in} - T_T)}{R_{sink}} \text{ ---------- } \textit{Equation 7}$$

Where R_{sink} is the thermal resistance of the heat sink. To simplify the analysis, the temperature across the top side of the TEM and the heatsink was assumed to be uniformly distributed with temperature T_T.

The heat being leaked in to the chamber through one wall is

$$Q_{leak} = \frac{T_{ambient} - T_{in}}{R_{wall}} \text{ ---------- } \textit{Equation 8}$$

where R_{wall} is the thermal resistance of the insulated wall.
Hence, using energy balance equation, change in T_{in} can be written as

$$C_{in}\left(\frac{dT_{in}}{dt}\right) = 5Q_{leak} - Q_L \text{ ---------- } \textit{Equation 9}$$

$$\therefore \frac{dT_{in}}{dt} = \left(\frac{1}{C_{in}}\right)\left\{\frac{5(T_{ambient} - T_{in})}{R_{wall}} - \frac{T_{in} - T_T}{R_{sink}}\right\} \text{ ---------- } \textit{Equation 10}$$

where $C_{in} = \rho V c_{air}$ is the thermal capacity of the air inside the chamber, given ρ is density of air and V is the volume of air inside.

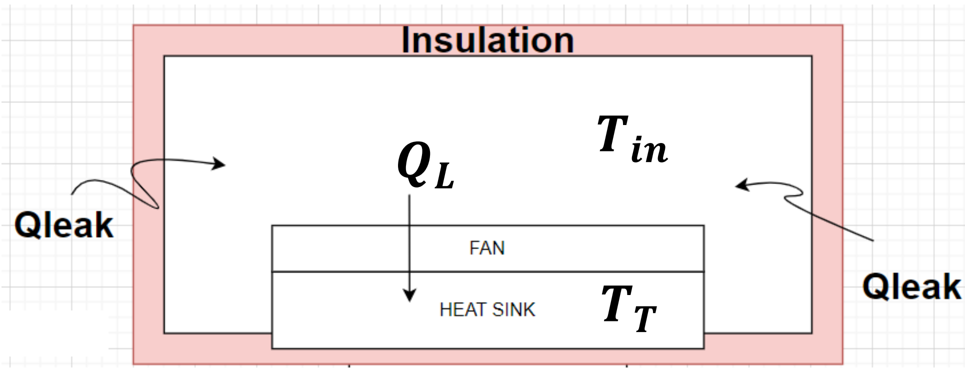

Figure 11: Schematic Representation of Chamber

4.2.2 Modelling Variation of T_T

The schematic shown in figure 12 illustrates the different heat entities that contribute to change in temperature T_T. In the figure, $Q_f^{B\to T}$ refers to the Fourier heat conduction form TEM bottom side to top side due the difference in temperature between the two faces of the module, $\frac{Q_J}{2}$ refers to the Joule heating and Q_P refers to the Peltier heat absorbed from the top side.

Hence, the energy balance for TEM top side can be expressed as [24]

$$\frac{dT_T}{dt} = \left(\frac{1}{C_T}\right)\left(Q_f^{B\to T} + Q_L - Q_p + \frac{Q_j}{2}\right) \text{ ---------- } \textit{Equation 11}$$

$$\therefore \frac{dT_T}{dt} = \frac{1}{C_T}\left\{\frac{K_m A}{L}(T_B - T_T) + \frac{1}{R_{sink}}(T_{in} - T_T) - S_m I T_t + \frac{I^2 R}{2}\right\} \text{ --------Equation12}$$

where C_T is the thermal capacity of TEM top side + top heat sink assembly, K_m is the thermal conductivity of the peltier element and S_m is the Seebeck coefficient.

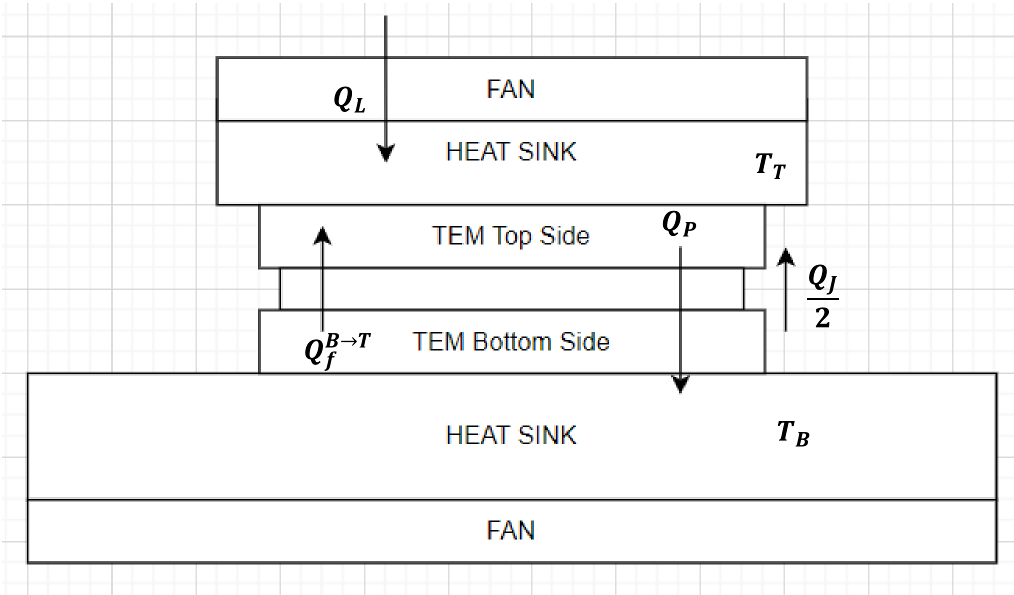

Figure 12: Schematic Representation of TEM+Heatsink+Fan Assembly

4.2.3 Modelling Variation of T_B

The schematic shown in fig 13 illustrates the different heat entities that contribute to change in temperature T_B. In the figure, $Q_f^{B \to T}$ refers to the Fourier heat conduction form TEM bottom side to top side due the difference in temperature between the two faces of the module, $\frac{Q_J}{2}$ refers to the Joule heating, Q_P refers to the Peltier heat absorbed from the top side and Q_{out} refers to the heat being dissipated out into the ambient by the bottom side heat sink + fan assembly.

$$\frac{dT_B}{dt} = \left(\frac{1}{C_B}\right)\left(-Q_f^{B \to T} + Q_p + \frac{Q_j}{2} - Q_{out}\right) \text{ ---------- Equation 13}$$

$$\therefore \frac{dT_B}{dt} = \frac{1}{C_B}\left\{\frac{-K_m A}{L}(T_B - T_T) + S_m I T_t + \frac{I^2 R}{2} - \frac{1}{R_{sink}}(T_B - T_{amb})\right\} \text{ ----------Equation 14}$$

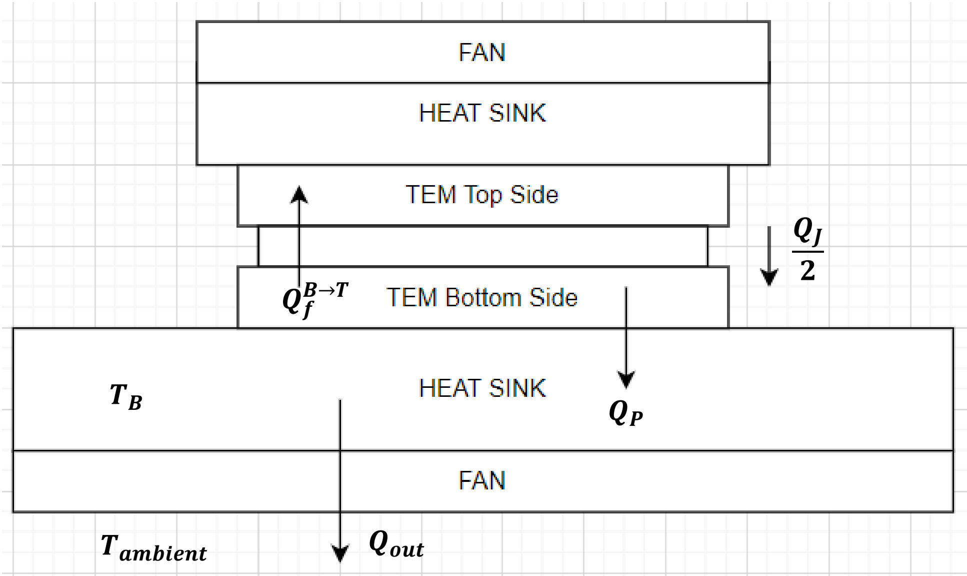

Figure 13: Schematic Representation of TEM+Heatsink+Fan Assembly

4.3 Model Implementation, Verification & Validation

The differential equations derived in section 4.2 were implemented in Simulink (refer Appendix B). Various parameters for each component of the plant were either obtained directly from datasheet or calculated using parameters mentioned in datasheet.

As mentioned earlier, the parameters of a thermoelectric module vary with temperature. However, in order to simplify the plant's model, these parameters were assumed to be constant over the working range. These temperature dependent parameters include seebeck coefficient (S_m), thermal conductivity (K_m) and internal resistance (R_m) of the module. These were calculated using formulae described in [12]. The parameters were calculates as follows

$$K_m = \frac{\left(\frac{V_{maxiumum} I_{maximum}}{\Delta T_{maximum}}\right)(T_h - \Delta T_{maximum})}{T_h} \text{ ---------- } Equation\ 15$$

$$R_m = \frac{\left(\frac{V_{maximum}}{I_{maximum}}\right)(T_h - \Delta T_{maximum})}{T_h} \text{ ---------- } Equation\ 16$$

$$S_m = \frac{V_{maximum}}{T_h} \text{ ---------- } Equation\ 17$$

Where K_m is the thermal conductivity of the individual thermocouple pellets in the module, R_m

is the internal resistance of the thermoelectric module, S_m is the Seebeck coefficient, $V_{maximum}$ is the maximum input voltage rated for the TEM module, $I_{maximum}$ is the maximum permissible current that can operate the module without fault, $\Delta T_{maximum}$ is the maximum temperature difference that can be obtained between the hot side and cold side of the TEM module, and T_h is the desired temperature of the hot side of the module.

Plugging in these values from the module's datasheet, the following values were obtained for these parameters

S_m (V/°C)	0.546
R_m(ohm)	3.05
K_m(W/°C)	0.00848

Table 2: Calculated parameters for TEM

4.3.1 Plant Verification and Validation

This is one of the most crucial steps to be done before carrying out the design of a controller. While verification refers to making sure each segment of the model is represented correctly and reflects how the actual system works, validation refers to exciting the plant with a known input and comparing the simulated and the actual outputs.

In order to verify the plant, the models for top surface of TEM, bottom surface of TEM, and that of the chamber were designed in Simulink as three separate subsystems which enhanced modularity and testability of the model (Refer Appendix B).

The following steps were followed to verify if the model:

- Functions as a heater and cooler as expected:
    - Input positive current to the model. Observe if T_{in} reduces and reaches a steady state value over time.
    - Observe if Q_{t_dot} (i.e. $\frac{dQ_T}{dt}$) starts from a negative value and increases to a steady state value over time.
    - Input negative current (direction of current reversed). Observe if T_{in} increases and reaches a steady state value over time.

- Observe if Q_{t_dot} (i.e. $\frac{dQ_T}{dt}$) starts from a positive value and decreases to a steady state value over time.

- Functions as cooler even in presence of a disturbance such as heating due to a heat source nearby:
  - Provide a step of 2°C to T_{amb} in chamber subsystem. The step should be such that it is initiated after 700 seconds. This simulates increase in Q_{leak} due to a nearby heat source.
  - Provide a step current input to the cooler/heater subsystem such that it increase current after 1700 seconds.
  - Observe T_{in}at the both time intervals.

To validate the model, the temperature inside the chamber was observed for different input voltages or currents using the actual hardware and the simulation model and then compared.

Section 5 consists of a comprehensive analysis of the results obtained in verification and validation steps.

4.4 Controller Implementation

In view of the non-linear behavior exhibited by the plant (as explained in section 1.4), a gain scheduled controller was designed for controlling the thermoelectric heater/cooler. Due to the complexity of the model, PID tuner in Simulink and Matlab were utilized to tune the gains for the controller.

Firstly, operating regions of the plant were obtained for the plant using the 'Model Linearizer' application in Simulink. By providing a desired state (desired T_{in}), the application linearizes the model at that point and returns a state-space model at that operating point. For testing, the model was linearized at 14°C and 18°C. The method is the same for other operating regions.

The following transfer functions were obtained at above mentioned operating points:

$$P_1(s)[at\ operating\ point\ 18°C] = \frac{-0.2035s-0.01313}{s^3+2.735s^2+0.1963s+0.001548}$$ ---------- *Equation 18*

$$P_2(s)[at\ operating\ point\ 14°C] = \frac{-0.03329s - 0.001917}{s^3 + 2.736s^2 + 0.2007s + 0.002673}$$ ---------- *Equation 19*

As the transfer functions are 3rd order systems, the PID tuner application in Simulink was used to simplify the tuning process. The objectives of less than 20% overshoot, less than +/-2°C steady state errors were met using the tuner application. The following PID gains were obtained for 0% overshoot and 0 steady-state error:

	At operating point 14°C	At operating point 18°C
P	-0.33746	-0.0824
I	-0.01452	0.00018
D	0	0
N (Filter Coefficient)	100	100

Table 3: PID tuned parameters at the two operating points

As D = 0 at both operating points, the individual controllers are effectively a PI controller.

Fig 14 depicts the architecture of the gain scheduled controller that was designed in Simulink.

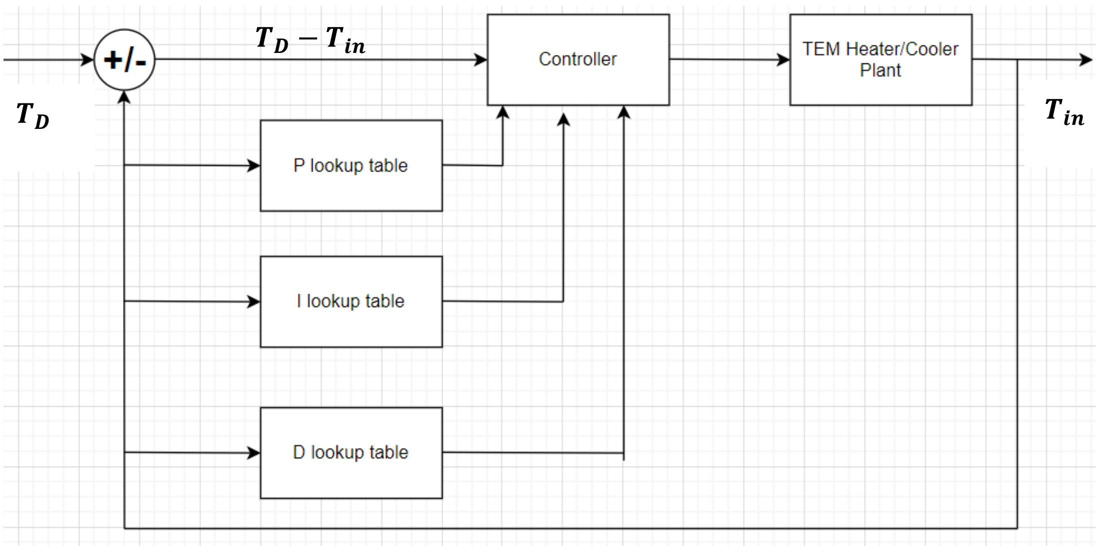

Figure 14: Block Diagram of the Designed Controller

The controller consists of lookup tables for gains P, I and D. The controller block is a master PID controller whose gains for P,I and D change based on the current operating point of, which is the temperature T_{in}. T_D is the desired chamber temperature.

Section 5.3 discusses the results for the implemented controller.

5 Results & Analysis

This section analyses the results that were obtained from simulating the mathematical model of the system and the controller that was designed.

Due to challenges in denoting subscripts in matlab, the variables used in the graph mean as follows:

- T_in → T_{in} (Temperature inside the heating/cooling chamber)
- T-t → T_T (Temperature of the top surface of the thermoelectric module)
- T-b → T_B (Temperature of the bottom surface of the thermoelectric module)
- Delta_T → $(T_B - T_T)$ = ΔT
- Qt-dot or Qt_dot → $\frac{dQ_T}{dt}$ (rate of change of energy on top surface of thermoelectric module)
- Qb-dot or Qb_dot → $\frac{dQ_B}{dt}$ (rate of change of energy on bottom surface of thermoelectric module)

5.1 Model Verification Results and Analysis

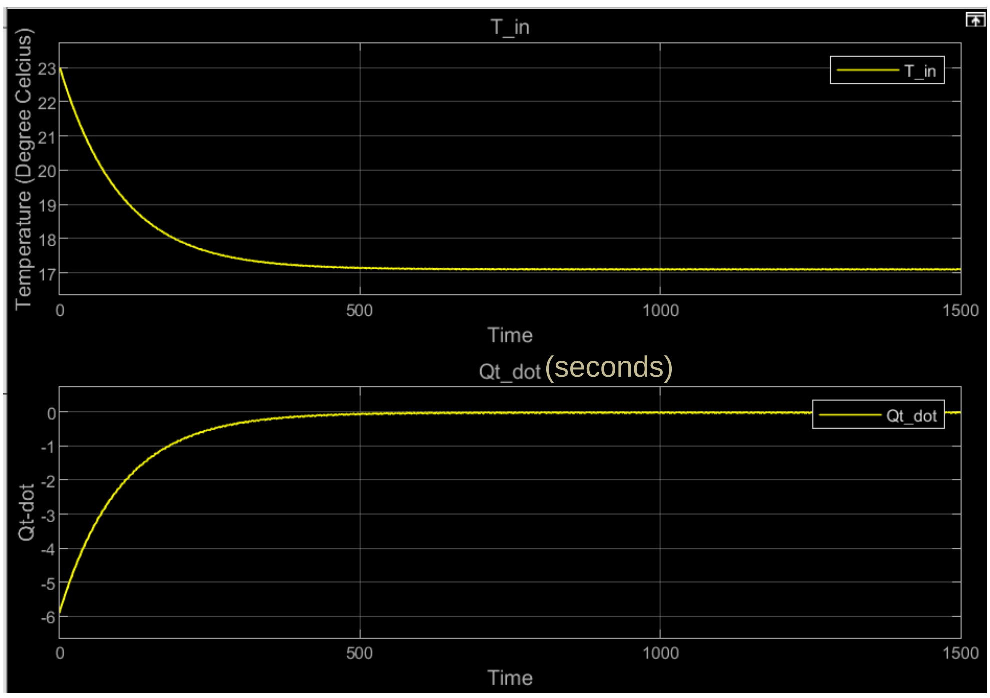

Figure 15: T_in v/s time & Qt_dot v/s time for Cooler

Figure 15 shows how the temperature inside the enclosure changes when current is applied to the system. In the figure, T_in refers to the temperature inside the chamber, which is the variable we are trying to control. Qt_dot is the rate of change of energy ($\frac{dQ_T}{dt}$) of the top surface of the thermoelectric module. The initial temperature of the box is same as the ambient, which is 23°C. When a positive current is applied to the system, the plant begins to behave as a cooler, hence T_in begins to lower over time and reaches a steady state value of 15°C. The negative value for Qt_dot simply means that the TEM is trying to remove heat from the inside of the enclosure. It starts with a more negative value and starts to become less negative over time as most of the heat in the chamber has been removed. When T_in reaches a steady state value, the system reaches equilibrium which means that the rate at which heat is being removed has been matched with the rate at which heat is being added to the chamber.

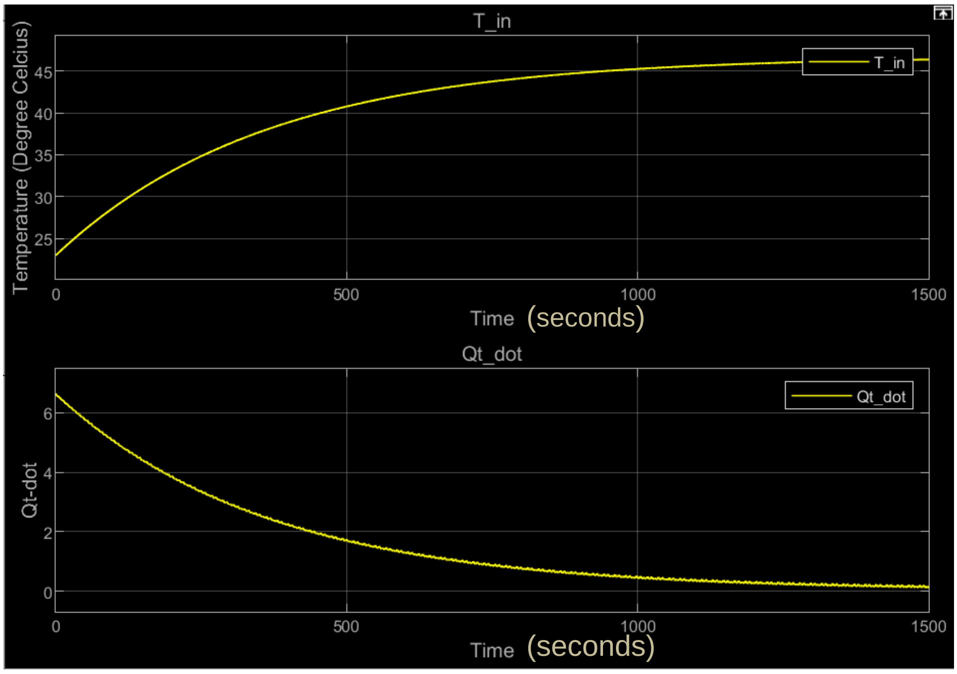

Figure 16: T_in v/s time & Qt_dot v/s time for Heater

To verify the model as a heater, a negative current is applied to the model, which translates to reversing the direction of current in the actual hardware. This makes the top surface of the thermoelectric module warm, hence heating the inside of the chamber. Figure 16 illustrates this where T_in begins to increase from ambient temperature of 23°C in the beginning to a steady state value of 45°C. Qt_dot starts with a positive value which indicates that the TEM is giving away heat into the inside of the chamber. Here again, Qt_dot reaches a steady state value as the heat being lost from the chamber into ambient equals the rate at which heat is being added into the system by the thermoelectric module.

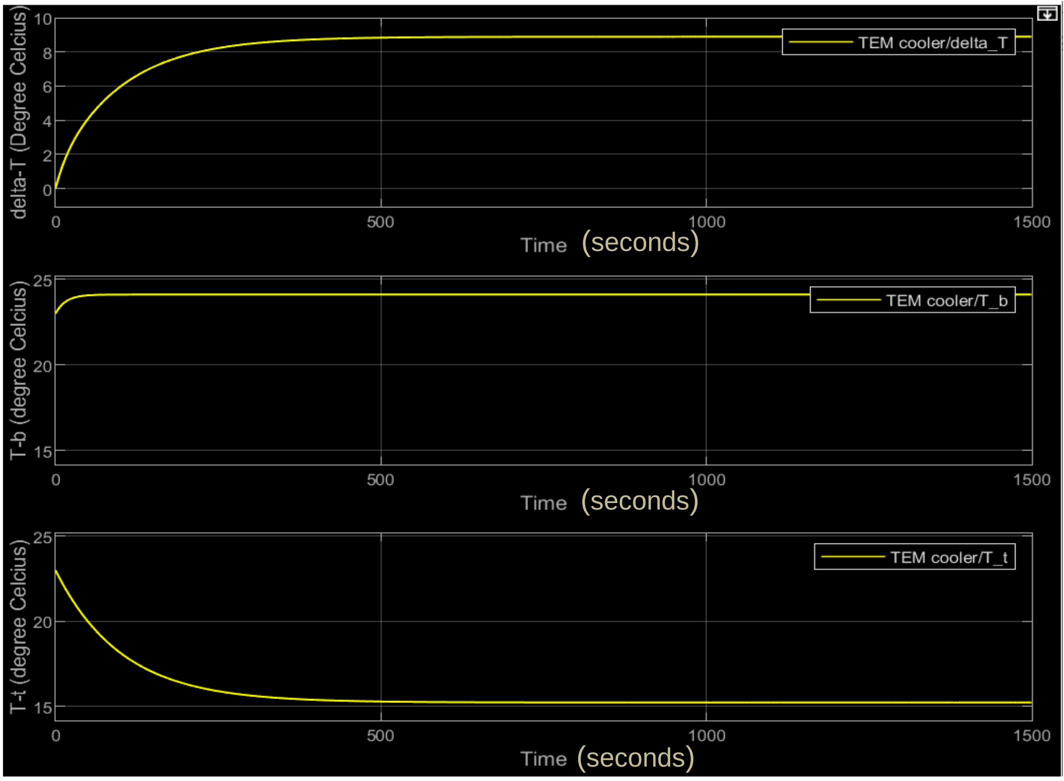

Figure 17: Top and Bottom Side Temperatures of TEM v/s Time(seconds) for Cooler

Figure 17 illustrates the temperature difference delta-T between the warm and cold surfaces of the TEM when functioning as a cooler. T-b denotes the temperature of the bottom surface while T-t denotes the temperature of the top surface. It is this temperature difference between the two surfaces that enables the thermoelectric module to function as a heat pump. Similarly, figure 18 shows the same but the curves for T-b and T-t are reversed when the system is operating as a heater. delta-T is negative since T-b < T-t.

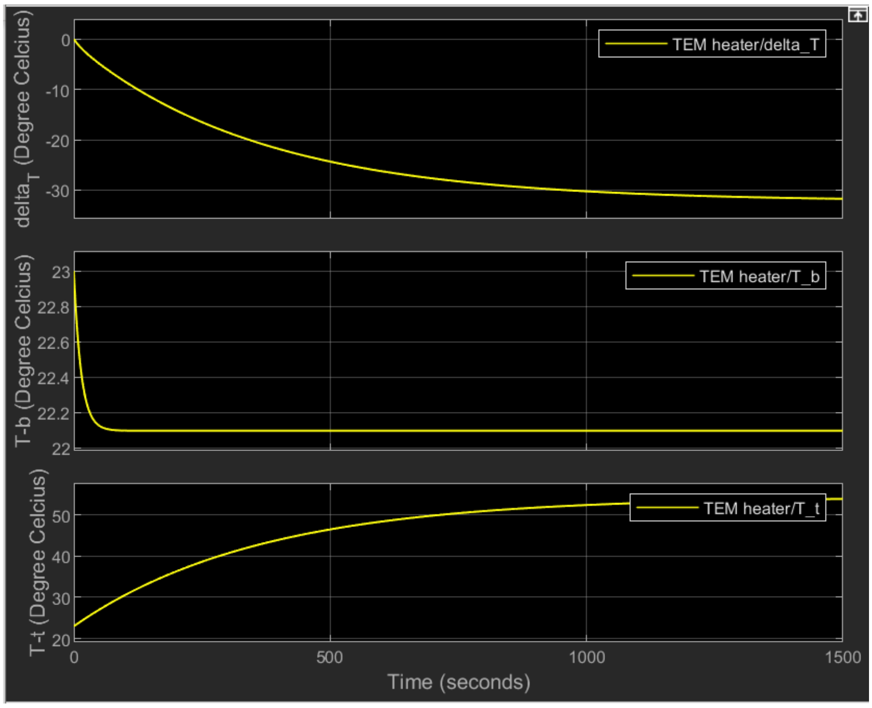

Figure 18: Top and Bottom Side Temperatures of TEM v/s Time(seconds) for Heater

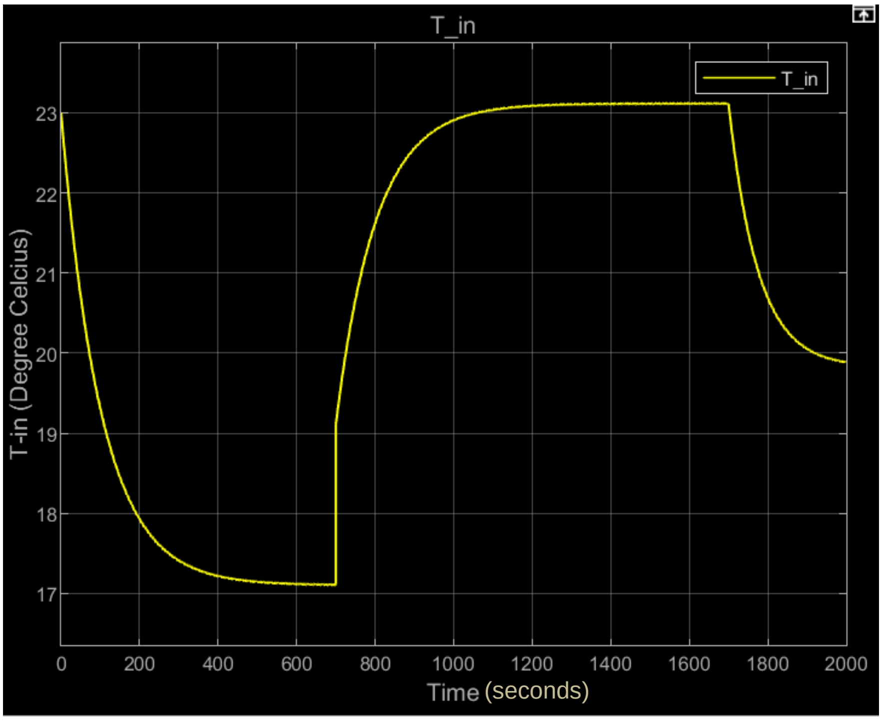

Figure 19: Effect of disturbance on open loop system (i.e. without a controller)

Figure 19 shows the effect of an external disturbance on the cooling chamber when the ambient temperature is suddenly raised by 2°C every time step after 700 seconds. It is also observed that the temperature began to drop when the current supplied to the device was increased at 1700 seconds. This shows the need for a controller to adjust the current and fend-off disturbances. The disturbance in ambient temperature modelled here can be viewed as a constant heat source in the vicinity of the temperature being turned ON at 700 seconds.

5.2 Model Validation Results and Analysis

The mathematical model was validated with the actual hardware by comparing the steady state temperatures of the inside of the chamber for different values of current in the cooling mode. Table 4 compares the temperatures inside the chamber as well as the top surface and bottom surfaces of TEM obtained from the model and the test hardware. An Arduino Uno coupled with DHT11 sensor was used to measure the ambient temperature inside the chamber. Digital thermometers were used to measure the temperature of the top and bottom surfaces of the TEM module.

Input Voltage V_{in} (V)	Steady State Current (A)	Actual Steady State Temperature Inside Chamber $T_{in_{actual}}$ (°C)	Steady State Temperature Inside Chamber Obtained from Model $T_{in_{model}}$ (°C)	Error $T_{in_{actual}}$ - $T_{in_{model}}$ (°C)
2	0.573	17	16.8	0.2
3	0.874	14	15.2	-1.2
6	1.765	8	14	-6

Table 4: Model Validation Result

The hardware could not have been tested for a much larger range due to limitations. Firstly, the maximum rated output voltage of the bench supply used for testing was 6V. Although there was an output for 12V, it could only supply a maximum of 1A. Hence, the hardware could not have been tested beyond 6V or for steady state temperatures below 14°C (considering test conditions during that time). Secondly, the resolution of the temperature sensor (DHT11) used was 1°C which meant the system could not be tested for minor temperature variations.

Nevertheless, from the data recorded, a maximum error of -6°C and minimum error or 0.2°C was observed. This proves that the mathematical model is a sufficiently good representation of the system given the number of assumptions that were considered in modelling such as not accounting for the effect of forced convection and dependence of TEM parameters on temperature.

Furthermore, although the cooler was observed to behave as a heater (instead of cooling) for very high values of positive current in the model, this can be explained by increased I^2R loss and uncertainties in modelling insulation properties of the chamber. This is depicted in figures 20 and 21. While T_{in} is at 13.87°C with 2A, it rose to 14.46°C with 3A.

This These results demonstrate the importance in considering the accuracy and trade-offs modelling certain aspects of a physical system. While we would be able to get a high fidelity model for the entire working range of the system, it may require accurate modelling of every small processes happening in the system, which can lead to complex differential equations and hence complicated controller design. However, if the model works for a limited working range even with unmodelled dynamics of a plant, it would lead to a much simpler controller design process.

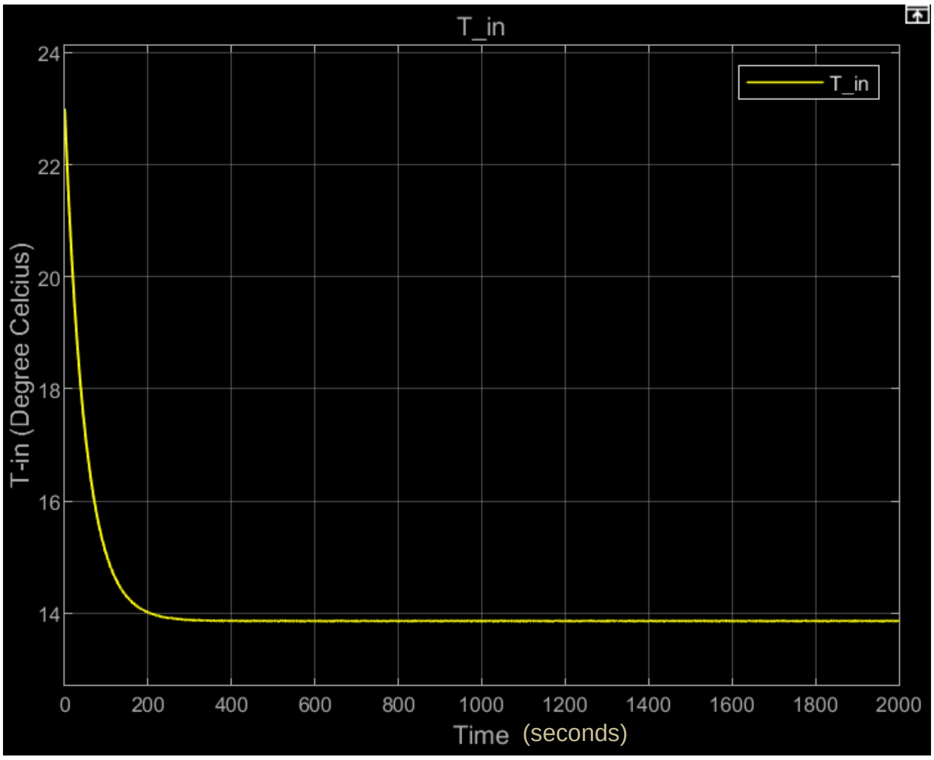

Figure 20 : T-in = 13.8°C at 2A current

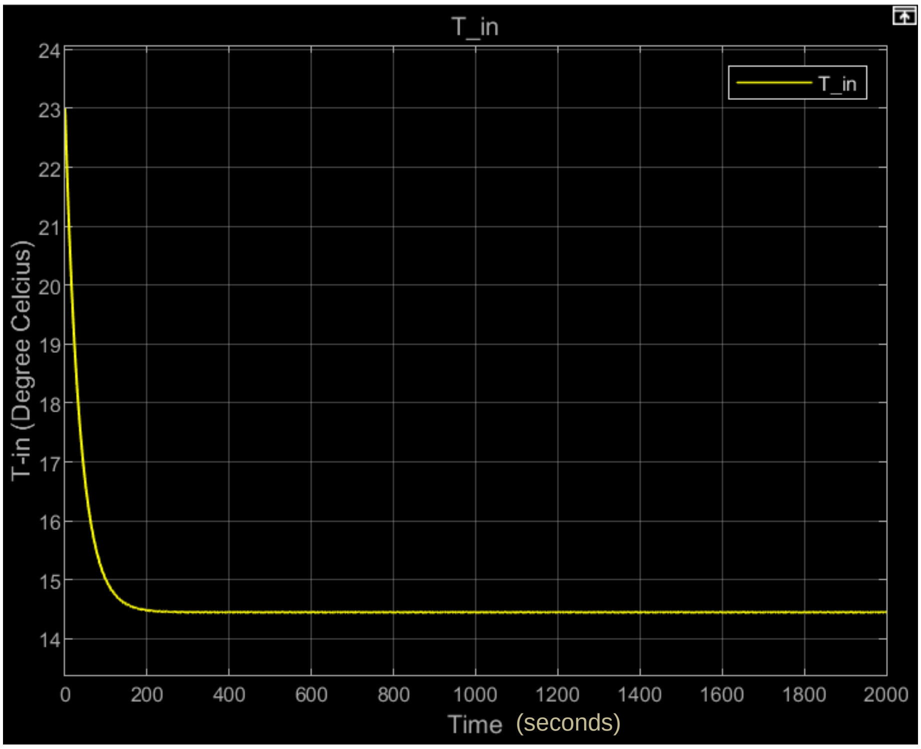

Figure 21 : T-in = 14.46°C at 3A current

5.3 Controller Performance Results and Analysis

A gain scheduled controller was designed for the range 15-40°C. The performance of the gain scheduled controller was well within the limits of 20% overshoot and +/- 2°C steady state error. With PID values as shown in table 3, 0% overshoot and 0 steady-state error was observed. Figure 22 shows the response that was obtained from the gain scheduled controller designed for the system. A step reference input was provided which was at 17°C (cooling mode) for upto 1500 seconds and then set to 20°C (heating mode). The controller was able to make the system track the reference temperatures in both, heating and cooling modes as shown in the figure.

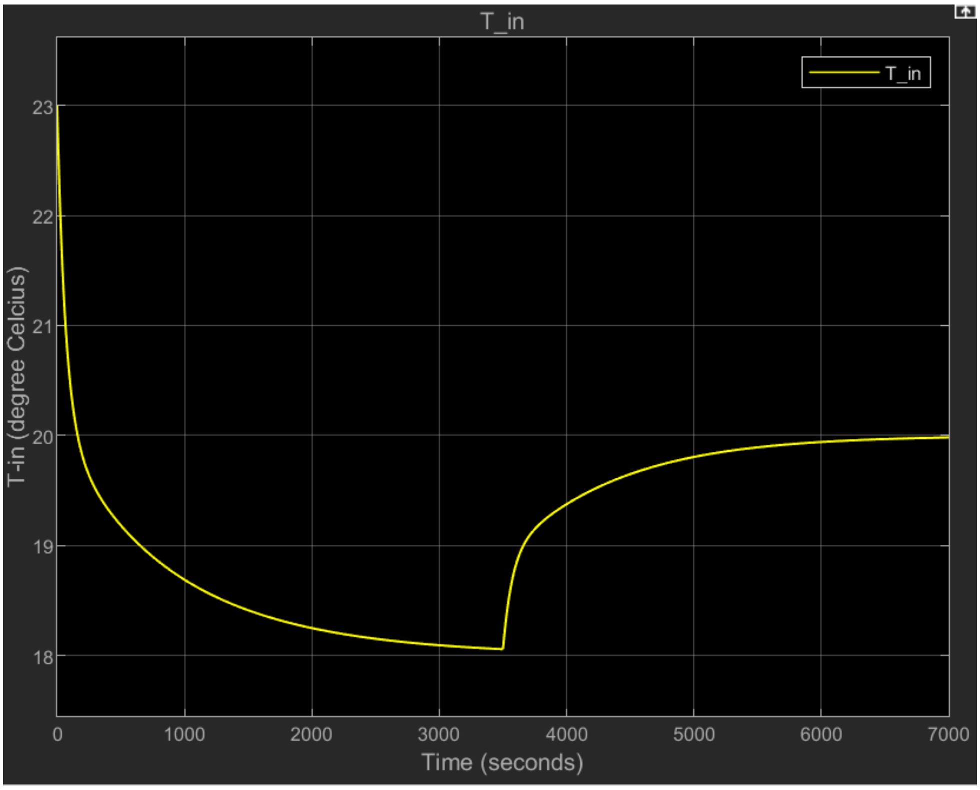

Figure 22 : Controller response for 2 reference temperatures

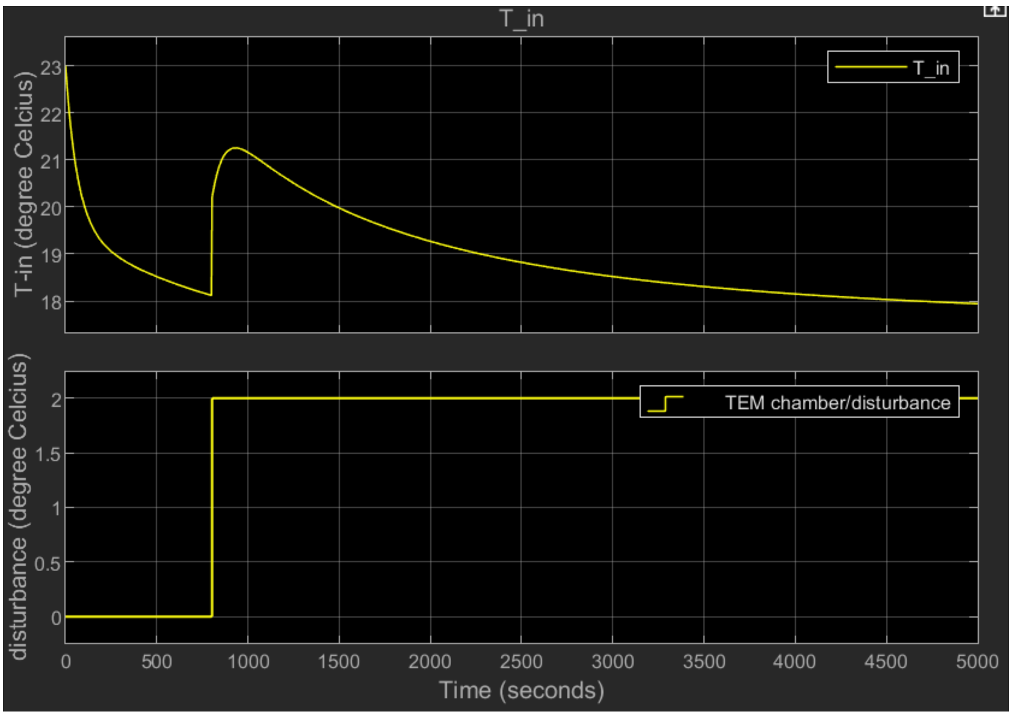

Figure 23 : Disturbance rejection capability in cooling mode

Figure 23 illustrates the controller's ability to compensate for any disturbances in the ambient temperature. A reference temperature of 18°C was given to the system. The system initially is able to bring down T_in to desired reference temperature without any disturbance. When a disturbance is given in the chamber, such as a heat source having temperature of 2°C, T_in rises suddenly and the controller is able to slowly compensate for the disturbance. T_in eventually goes down to the desired temperature.

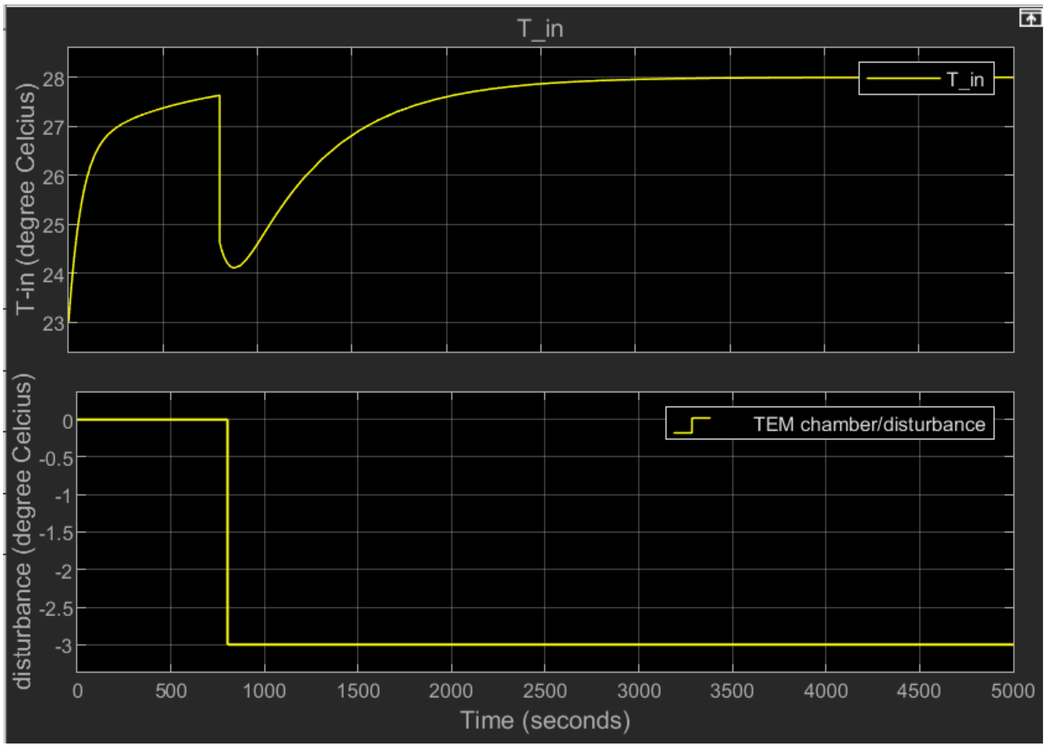

Figure 24 : Disturbance rejection capability in heating mode

Figure 24 demonstrates the controller's ability to reject disturbance in heating mode. The disturbance can be imagined as a scenario where the system suddenly begins to lose heat causing the temperature to drop by 3°C. The controller is able to compensate for this and heat the chamber back to 28°C.

6 Further Work

There are multitude of opportunities with respect to both, the TEM heater/cooler and GUSTAVO. The following list provides a summary on what could be tried and achieved. Most of these ideas evolved through experimentation over the course of the project. Hence, while some of these ideas can be seen as an additional functionality, others can also be seen as suggestions for improvements to current design and the system. The following are a few suggestions on future work:

- Many assumptions were considered when the system was modelled. There are scopes of improving the model by adding the dynamics due to forced convection due to the heatsink+fan assembly on top and the bottom sides of the system. Other dynamics that could be considered include adding temperature dependency for the parameters of the TEM module, specifically its seebeck coefficient (S_m), thermal conductivity (K_m) and module resistance (R_m).
- There is scope for a more compact and efficient design to cool a microplate. A design that is worth trying would be to make a case with single aluminium block that can fit a microplate perfectly in it. The case will be such that it covers the sides and bottom of the microplate, leaving only its top exposed to ambient. The base of the case would be directly attached to the ceramic surface of the TEM. However, it would not be possible to heat the microplate as heating would require a heatsink on top of the host surface of the TEM module.
- For faster performance, multiple TEM modules could be used.
- A sliding mode controller would be a suitable control system for a TEM heater/cooler. This is due to its immunity from continuously varying plant parameter values. However, the trade-off is a complex design and analysis procedure.
- A robotic arm for GUSTAVO to handle a large batch of microplates so that it is truly automated.
- A centrifuge could be developed for GUSTAVO.
- Would be worthwhile to study the feasibility of using optical feedback linear actuator to move the piston used in the pipette.

References

[1] P. E. Gray, The Dynamic Behavior of Thermoelectric Devices, Hassell Street Press, 2021.

[2] S. Patidar, “Applications of Thermoelectric Energy: A Review,” *International Journal for Research in Applied Science and Engineering Technology,* vol. 6, pp. 1992-1996, 2018.

[3] M. Jiang, “An Overview of Radioisotope Thermoelectric Generators,” Stanford University, 15 March 2013. [Online]. Available: http://large.stanford.edu/courses/2013/ph241/jiang1/. [Accessed 13 July 2023].

[4] S. a. W. J. Song, “Dynamic Model of Thermoelectric Cooler and Temperature Control Based on Adaptive Fuzzy-PID,” *Applied Mechanics and Materials,* Vols. 130-134, 2011.

[5] T. L. Nataporn Korprasertsak, “Mathematical modeling and validation of cooling/heating effects in thermoelectric module coupled with heat sinks,” in *2016 7th International Conference on Mechanical and Aerospace Engineering (ICMAE)*, London, 2016.

[6] D. F. a. P. F. M. a. P. F. M. a. S. A. a. A. T. A. a. H. I. P. a. F. I. W. Sundayani and Sinulingga, “PID temperature controlling of thermoelectric based cool box,” in *2017 International Conference on Control, Electronics, Renewable Energy and Communications (ICCREC)*, Yogyakarta, Indonesia, 2017.

[7] D. Z. a. G. Tan, “A review of thermoelectric cooling: Materials, modeling and applications,” *Applied Thermal Engineering,* vol. 66, no. 1359-4311, pp. 15-24, 2014.

[8] R. a. E. H. Gouws, “A review on thermoelectric cooling modules: Installation design, performance and efficiency,” *Scientific research and essays,* vol. 8, pp. 485-492, 2013.

[9] A. a. A. T. a. R. M. Nugroho, “PID Controller Implementation For Temperature Control In Leakage Current Test Chamber 20kv Insulator,” *International Journal of Advanced Engineering Research and Science,* vol. 8, pp. 106-112, 2021.

[10] H. Lee, Thermal Design, Heat Sinks, Thermoelectrics, Heat Pipes, Compact Heat Exchangers, and Solar Cells, Michigan: John Wiley & Sons, 2022.

[11] H. Goldsmith, Thermoelectric Refrigeration, Plenum Press, 1964.

[12] S. a. B.-y. S. Lineykin, “Modeling and Analysis of Thermoelectric Modules,” *Industry Applications, IEEE Transactions on,* vol. 43, pp. 505 - 512, 2007.

[13] J. A. O. J. S. A. T. M. J. G. J. A. Chavez, “SPICE model of thermoelectric elements including thermal effects,” in *Proceedings of the 17th IEEE Instrumentation and Measurement Technology Conference* , Baltimore, 2002.

[14] D. Incropera, Fundamentals of Heat and Mass Transfer, John Wiley & Sons, 2002.

[15] W. J. P. III, Modelling, Analysis, and Control of Dynamic Systems, Wiley, 1999.

[16] R. A. M. M. M. O. M. J. Shirafkan, “Design and implementation of a nonlinear controller for thermal cycler with application to DNA amplification,” *Transactions of the Institute of Measurement and Control,* vol. 38, no. 3, pp. 293-304, 2016.

[17] M.Gopal, “Nonlinear System Analysis,” in *Control Systems Principles and Design*, New Delhi, McGraw Hill Education, 2016, pp. 788-834.

[18] T. N. a. T. Leephakpreeda, “Control of Metal Hydride Reactor Coupled with Thermoelectric,” in *2013 IEEE/ASME International Conference on Advanced Intelligent Mechatronics*, Wollongong, 2013.

[19] F. B. a. U. B. a. M. S. a. T. Schirmeister, “FINDUS: An Open-Source 3D Printable Liquid-Handling Workstation for Laboratory Automation in Life Sciences,” *SLAS Technology,* vol. 25, no. 2472-6303, pp. 190-199, 2020.

[20] B. H. a. C. Duang, “System dynamic model and temperature control of a thermoelectric cooler,” *International Journal of Refrigeration,* vol. 23, no. 0140-7007, pp. 197-207, 2000.

[21] C. G. J. B. A. L. J. Fernández de Cañete, Automatic Control Systems in Biomedical Engineering, Springer, 2018.

[22] M. Driels, Linear Control System Engineering, Singapore: McGraw Hill International Editions, 1996.

[23] J. D. P. A. E. N. Gene F. Franklin, Feedback Control of Dynamic Systems, Pearson, 2015.

[24] E. E. a. R. S. a. R. v. G. a. B. d. J. a. T. Oomen, “Thermoelectric modules in mechatronic systems: Temperature-dependent modeling and control,” *Mechatronics,* vol. 79, no. 0957-4158, p. 102647, 2021.

[25] D. a. L. W. Leith, “Survey of gain-scheduling analysis and design,” *Int. J. Control,* vol. 73, pp. 1001-1025, 2000.

[26] “Model Gain-Scheduled Control Systems in Simulink,” MathWorks, [Online]. Available: https://uk.mathworks.com/help/control/ug/set-up-simulink-models-for-gain-scheduling.html. [Accessed 10 June 2023].

[27] “Adaptive Peltier Module, 58.6W, 6A, 15.7V, 40 x 40mm,” [Online]. Available: https://uk.rs-online.com/web/p/peltier-modules/4901531. [Accessed 25 May 2023].

[28] D. W. B. L. Incropera, “Introduction to Conduction,” in *Fundamentals of Heat and Mass Transfer*, John Wiley & Sons, 2007, pp. 57-81.

Appendices

Appendix A

A.1 Gain Scheduled Control Modelled in Simulink

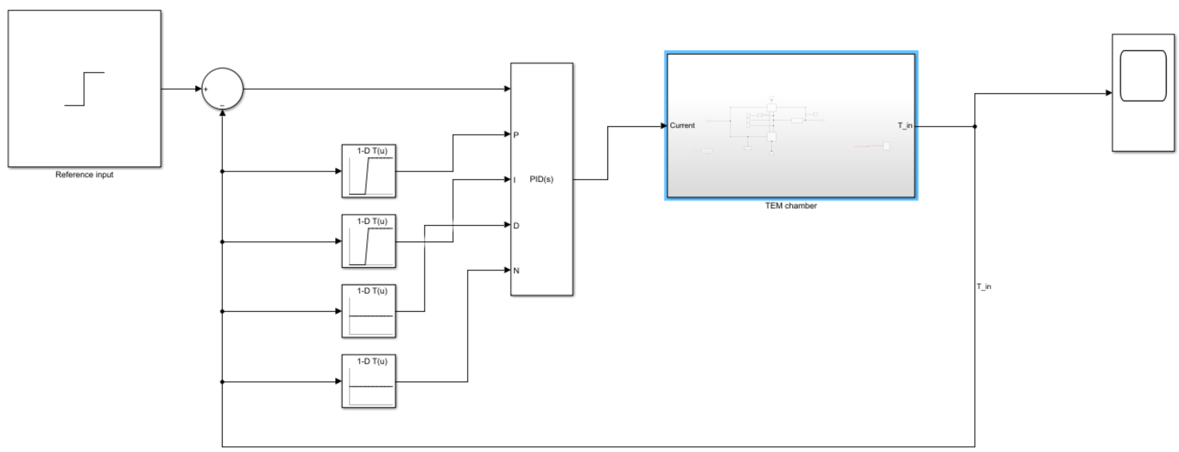

Appendix B

B.1 Simulink Model of Heater/Cooler

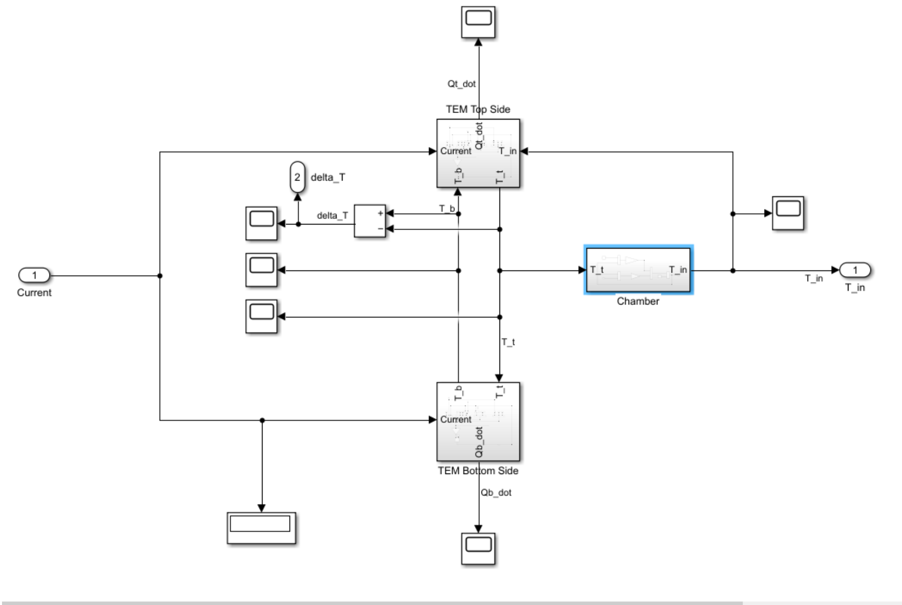

B.2 Simulink Model of TEM Top Side

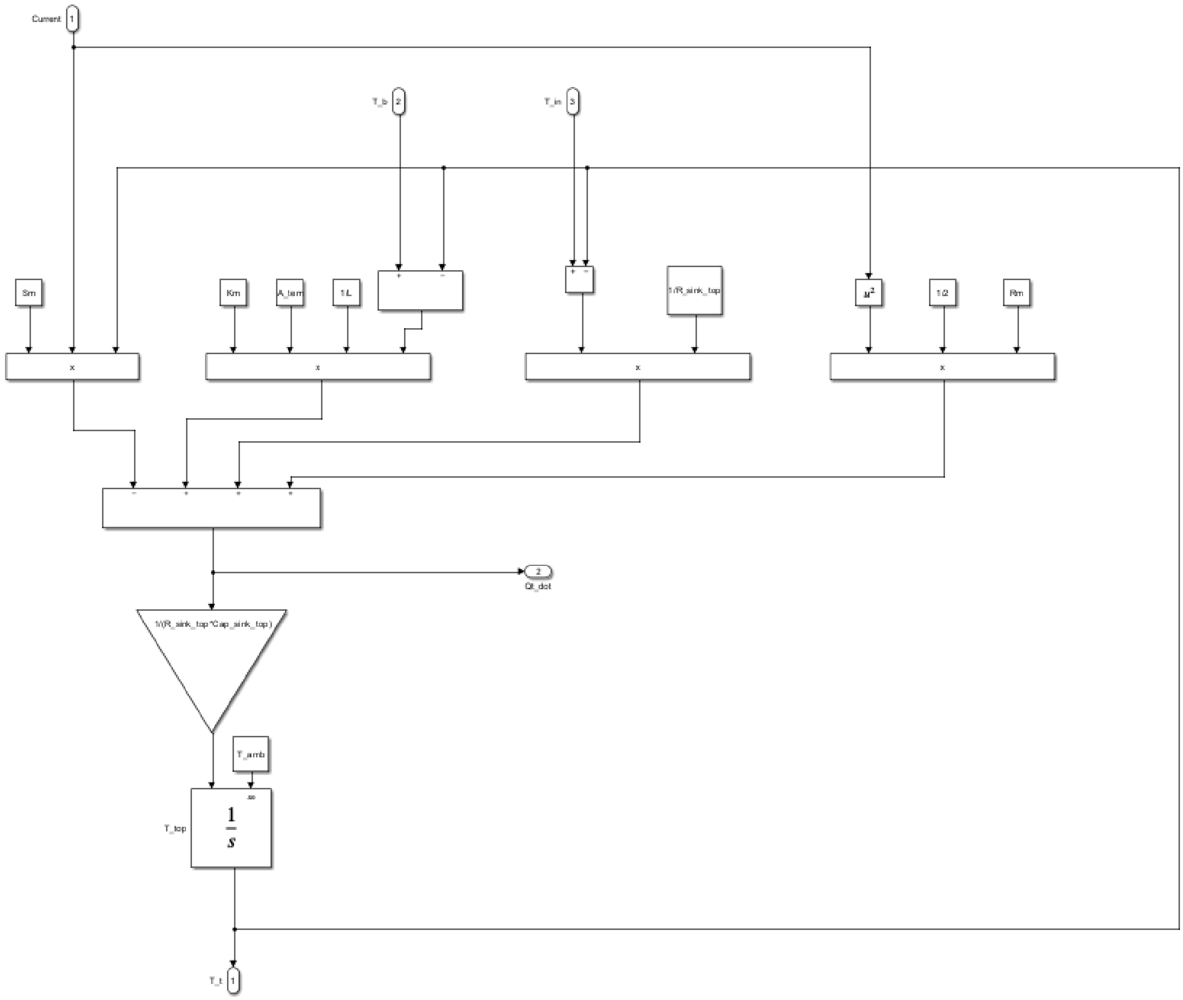

Current
1
T_b
2
T_in
3
Sm
Km
A_tem
1/L
1/R_sink_top
u^2
1/2
Rm
2
Qt_dot
1/(R_sink_top*Cap_sink_top)
T_amb
T_top
$\frac{1}{s}$
T_t
1

B.3 Simulink Model of TEM Bottom Side

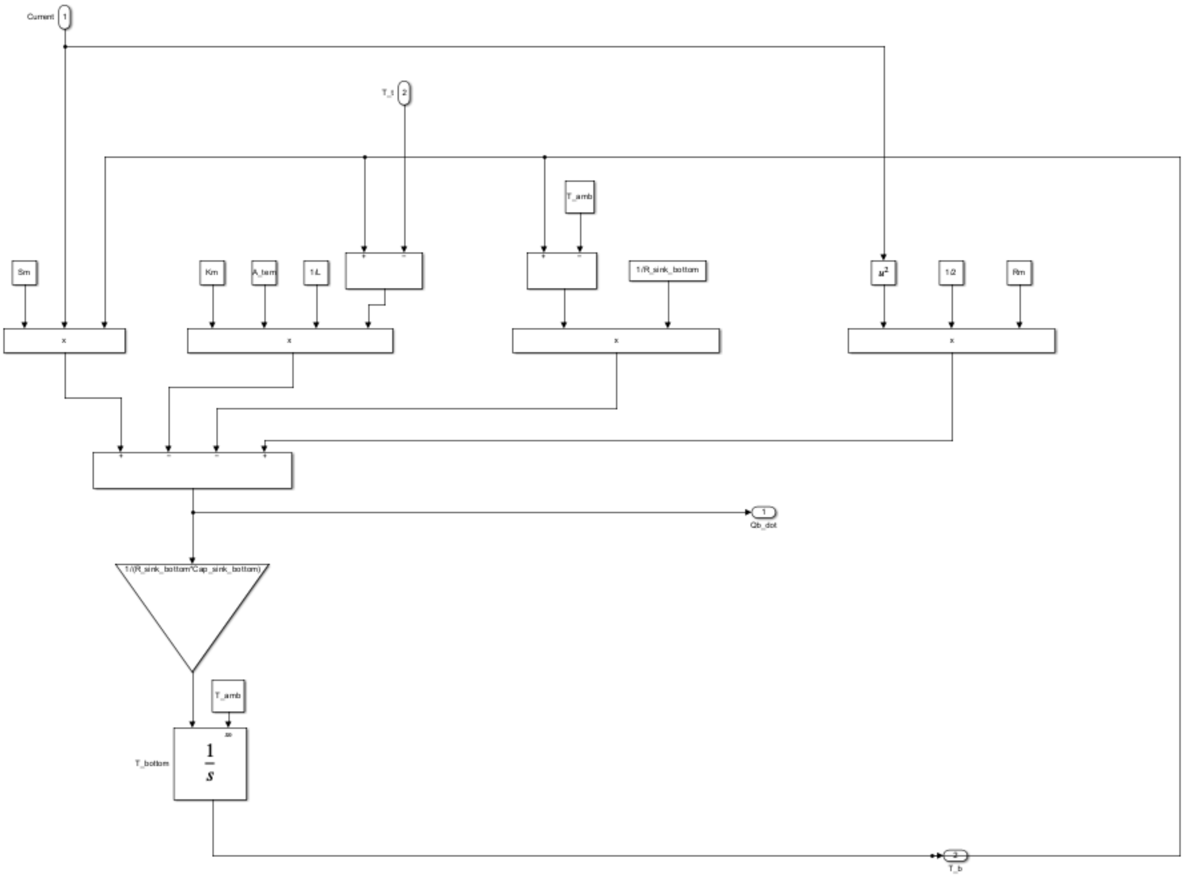

B.3 Simulink Model of Chamber

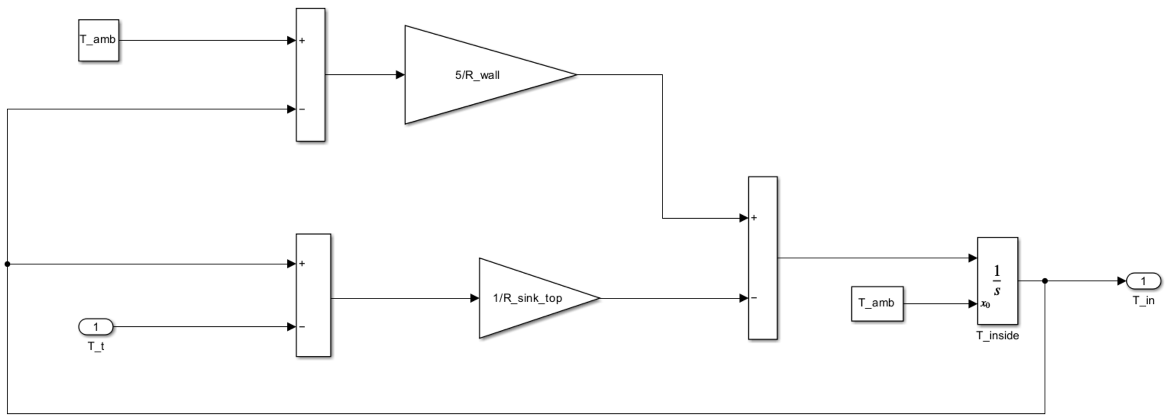

Appendix C

C.1 Matlab Script Containing Model Parameters

```
%% Top heat sink
m_sink_top = 0.170; % Kg
R_sink_top = 0.5; % degC/W

% Specific heat capacity for 6035-T5 Aluminium
% Ref: https://www.matweb.com/search/DataSheet.aspx?MatGUID=79875d1b30c94af39029470988004fb6&ckck=1
c_sink_top = 0.9e3; % J/Kg.degC

Cap_sink_top = m_sink_top*c_sink_top; % Thermal capacitance of top heat sink

%% Bottom heat Sink

m_sink_bottom = 0.650; % Kg
R_sink_bottom = 0.16; % degC/W

% Specific heat capacity for 6035-T5 Aluminium
% Ref: https://www.matweb.com/search/DataSheet.aspx?MatGUID=79875d1b30c94af39029470988004fb6&ckck=1
c_sink_bottom = 0.9e3; % J/Kg.degC

Cap_sink_bottom = m_sink_bottom*c_sink_bottom; % Thermal capacitance of top heat sink

%% Environmental conditions

T_amb = 23; % Ambient Temp degC

%% Enclosure Specifications
```


```
T_amb = 23; % Ambient Temp degC
```


```
%% Enclosure Specifications

V = 0.065*0.135*0.095; % Volume of cube (m-3).
rho = 1.2983; % Density of air (kg/m-3)
c_air = 1.87e3; % Specific heat capacity of air (J/Kg.degC). Ref: https://www.withouthotair.com/cI/page_334.shtml#:~:text=Heat%20capaciti
w = 10e-3; % wall thickness (m)
A_wall = 0.135*0.095; % Area of wall (m-2). Need to change. This is test value
k_wall = 0.1; % Thermal conductivity of XPS (W/m-degC)

R_wall = (w/(k_wall*A_wall)); % Total thermal resistance of walls
%% TEM Specifications

Sm = 0.546; % Seebeck Coefficient (V/degC)
Rm = 3.05; % TEM resistance (ohm)
Km = 8.48e-3; % TEM Thermal conductance (W/degC)
n = 254; % Number of pellets
A_tem = 0.001^2; % Surface area of each face of TEM module (m-2)
L = 2e-3; % Height of pellet

%% COntrol surface surrounding hot side

V_control = 0.3^3; %Volume of cube (m-3). Need to change. This is test value
```